IEEE Access
Multidisciplinary | Rapid Review | Open Access Journal

Received October 21, 2017, accepted December 11, 2017, date of publication December 18, 2017, date of current version June 29, 2018.

Digital Object Identifier 10.1109/ACCESS.2017.2784407

Mitigation of Power System Forced Oscillations: An E-STATCOM Approach

SHUANG FENG[1], XI WU[1], PING JIANG[1], LE XIE[2], (Senior Member, IEEE), AND JIAXING LEI[1], (Member, IEEE)

[1]School of Electrical Engineering, Southeast University, Nanjing 210096, China
[2]Department of Electrical and Computer Engineering, Texas A&M University, College Station, TX 77845, USA

Corresponding author: Shuang Feng (sfeng@seu.edu.cn)

This work was supported in part by the National Natural Science Foundation of China under Grant 51577032, in part by the NSF under Grant ECCS-1760554 and Grant 1150944, and in part by the Qatar National Research Fund.

ABSTRACT With the integration of renewable energy resources and variable loads into power grid, power oscillations caused by persistent external fluctuating forces are becoming more prevalent. Termed as ''forced oscillations (FO)'', such phenomena could happen even when the grid is with good damping characteristics. Therefore, conventional mitigation methods based on improving damping are rendered less effective. By leveraging the new control capability offered by static synchronous compensator with energy storage (E-STATCOM), a novel approach to mitigate FOs is proposed in this paper. A control strategy based on resonant controllers is adopted to modulate active and reactive power supplied by E-STATCOM. It is theoretically shown that FOs propagating from the disturbed area to other areas can be effectively eliminated by this method. Besides, we derived the analytical relationship among the location, the capacity of E-STATCOM and the suppression performance. Case studies demonstrate the effectiveness of the proposed method.

INDEX TERMS Forced oscillations, mitigation, STATCOM, energy storage, resonant controller, active and reactive power control.

I. INTRODUCTION

Recently, the increasing occurrence of power oscillations caused by persistent external fluctuating forces has drawn the attentions of power system operators and researchers [1]–[4]. Termed as ''forced oscillations (FO)'', they have happened in China, America and Canada and usually last for minutes or even hours, which endanger the stability of grid and damage the devices [5], [6]. Moreover, it has been observed that if the frequency of the oscillations is close to the natural frequency of grid, resonance phenomena could happen which lead to large amplitude of power oscillations and could even result in cascade blackout [2].

It should be noted that although the waveforms of FOs look similar to the weak damping oscillations (WDO), their root causes and countermeasures are completely different [3]. The primary reason for WDOs is the low or even negative damping of the system [7], [8]. By contrast, the FOs are introduced into the system by external fluctuation forces, which could be mechanical power variation from hydro or wind turbine, the demand fluctuations and etc. [9]–[13]. For instance, the FOs event happened in western American power system in 2013 was caused by the vortex related mechanical turbine oscillations of the hydro plants [2]. Given the increasing penetration of renewables, it is likely to see many more FOs in the system.

After the detection of FOs [1], [3], proper countermeasures should be taken. According to the cause of FOs, the most intuitive method would be removing the external fluctuation forces. However, two main reasons limit its implementation in power grid. On one hand, removing the disturbance relies on accurate online localization method. Yet, with current online localization methods, such as graph-theoretic techniques and hybrid-dynamic simulation method [4], [14], [15], it is hard to localize exactly and timely. On the other hand, the source could be a small disturbance or in some important power plant or load, which is neither practical nor economical to remove. Also, improving the damping with PSS and FACTS-based stabilizers is suggested by some papers to mitigate FOs [16]. Unlike WDOs, which will attenuate quickly by increasing the damping of system, FOs still happen and sustain with the appearance of external fluctuation forces even the system is with good damping

characteristics [2]. Therefore, real-time mitigation of FOs needs to be investigated.

Static synchronous compensator (STATCOM) has been applied in power system to suppress power oscillations, but its mitigation ability is limited by the the restriction of voltage amplitude [17], which makes it less powerful for FOs driven by persistent external forces. By incorporating an energy storage unit into STATCOM, a more flexible device E-STATCOM is obtained, which increases the control degrees of freedom and hence provides a possible solution for forced oscilltions [17]–[19]. Leveraging E-STATCOM's unique capability of supplying both active and reactive power in real-time, we propose a control algorithm to fully mitigate the FOs. In this approach, resonant controllers [20]–[22] are adopted to generate the power needed to be injected into the system. With the proposed method, the FOs propagating from the disturbed generator/area to the rest of power grid can be eliminated timely and in turn, the FOs of the disturbed generator/area are also reduced.

This paper is organized as follows. Section II establishes the model of the single-machine infinite-bus (SMIB) system with E-STATCOM, based on which the principle of FOs is presented. Section III elaborates the proposed method in a general power system and investigates the analytical relationship between the capacity and location of E-STATCOM. In Section IV, case study results in both single-machine and multi-machine system are shown to validate the proposed method. Conclusions and possible future research directions are presented in Section V.

II. MATHEMATICAL FORMULATION OF FORCED OSCILLATIONS

A. SYSTEM MODELING

In this section, we describe the modeling and control of FOs in power systems. A SMIB system with E-STATCOM shown in Fig. 1 is adopted, where the disturbed generator/area of FOs is represented by a synchronous generator and the FOs flow through a transmission line to the rest of the system represented by an infinite bus. E-STATCOM is installed between the disturbed generator/area and the infinite bus. The classic second order model of generator is adopted, which is composed of voltage source and transient reactance. In Fig. 1, E_g and δ_g denote the amplitude and phase angle of voltage source, respectively. The voltage amplitude and phase angle of the infinite bus are E_b and 0, separately. The reactance between the voltage source and E-STATCOM is X_g:

$$X_g = X_d' + X_t + X_L \tag{1}$$

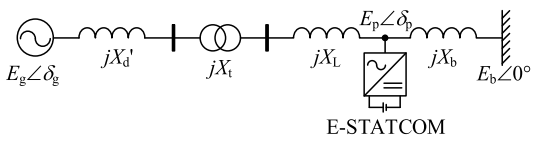

FIGURE 1. SMIB system with E-STATCOM.

where X_d', X_t and X_L are the transient reactance of generator, the leakage reactance of transformer and equivalent reactance between transformer and E-STATCOM, respectively. The reactance between E-STATCOM and the infinite bus is X_b, then the electrical location of E-STATCOM is defined as a:

$$a = \frac{X_g}{X_g + X_b} \tag{2}$$

The theoretical range of a is [0, 1]. The smaller a is, the closer E-STATCOM is to the generator.

The equivalent circuit of Fig. 1 is shown in Fig. 2, where E-STATCOM is modeled as a current source supplying active and reactive power P_{inj}, Q_{inj} to the network. P_g and Q_g are the active and reactive power flowing from the generator to the bus connected with E-STATCOM. P_b and Q_b are the active and reactive power flowing to the infinite bus.

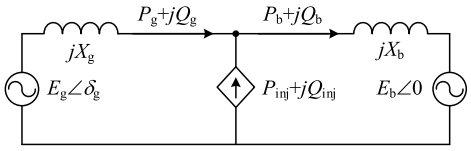

FIGURE 2. Equivalent circuit of SMIB system with E-STATCOM.

The linearized equation of motion for small-signal analysis is [23]

$$\begin{cases} M\dfrac{d\Delta\omega_g}{dt} = \Delta P_m - \Delta P_e - D\Delta\omega_g \\ \dfrac{d\Delta\delta_g}{dt} = \omega_b\Delta\omega_g \end{cases} \tag{3}$$

where M, δ_g and ω_g are the inertia, power angle and rotor speed of the generator, respectively. P_m is the mechanical power output, D denotes the damping coefficient, ω_b is the base angle electrical speed and ω_g is in per unit scale. Δ represents the small perturbations in the corresponding variables.

Inspired by [17], ΔP_g can be expressed as:

$$\Delta P_g = K_P\Delta\delta_g - \Gamma_P P_{inj} - \Gamma_Q Q_{inj} \tag{4}$$

where the expressions of K_P, Γ_P and Γ_Q in SMIB system with E-STATCOM are further derived by this paper.

$$K_P = \frac{E_{g0}E_{b0}\cos\delta_{g0}}{X_g + X_b} \tag{5}$$

$$\Gamma_P = \frac{(1-a)^2 E_{g0}^2 + (1-a)\,aE_{g0}E_{b0}\cos\delta_{g0}}{E_{p0}^2} \tag{6}$$

$$\Gamma_Q = -\frac{a\,(1-a)\,E_{g0}E_{b0}\sin\delta_{g0}}{E_{p0}^2} \tag{7}$$

where the subscript 0 represents the value of the corresponding variable at steady state. Similar to the derivation of (4)-(7), the expression of the reactive power ΔQ_g can be obtained:

$$\Delta Q_g = K_Q\Delta\delta_g - \Phi_P P_{inj} - \Phi_Q Q_{inj} \tag{8}$$

where the coefficients K_Q, Φ_P and Φ_Q are derived and denoted as

$$K_Q = \frac{E_{b0}E_{g0}\sin\delta_{g0}}{X_g + X_b}(1-2a) \tag{9}$$

$$\Phi_P = -\frac{a(1-a)E_{g0}E_{b0}\sin\delta_{g0}}{E_{p0}^2} \tag{10}$$

$$\Phi_Q = -\frac{(1-a)^2E_{g0}^2 - a^2E_{b0}^2}{2E_{p0}^2} - \frac{4a-3}{2} \tag{11}$$

According to Fig. 2, the active and reactive power ΔP_b and ΔQ_b flowing to the infinite bus are expressed as

$$\Delta P_b = \Delta P_g + P_{inj} \tag{12}$$

$$\Delta Q_b = \Delta Q_g + Q_{inj} \tag{13}$$

The model of SMIB system with E-STATCOM is obtained from (3)-(13) and the block diagram is shown in Fig. 3.

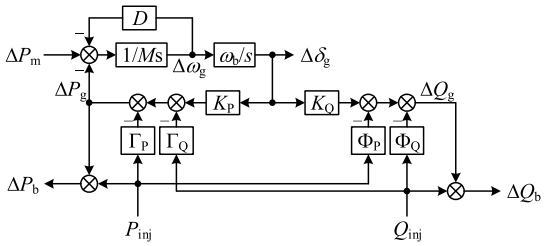

FIGURE 3. Block diagram of SMIB system with E-STATCOM.

The parameters K_x, Γ_x, and Φ_x (x = P, Q) represent the influences of $\Delta\delta_g$, P_{inj} and Q_{inj} on the active power ΔP_g and the reactive power ΔQ_g flowing from the generator to the bus connected with E-STATCOM. Γ_P and Φ_Q are two important parameters in this approach. Ignoring the voltage drop on the transmission line, (6) and (11) can be simplified as (14) with consideration that cos δ_{g0}, the power factor of generator, is approximate to 1.

$$\Gamma_P \approx \Phi_Q \approx 1 - a \tag{14}$$

(14) indicates that the ability of P_{inj} to influence ΔP_g is almost the same with that of Q_{inj} to influence ΔQ_g. Since the theoretical range of a is [0, 1], Γ_P and Φ_Q decline linearly from 1 to 0 with the increase of a according to (14). Therefore, the larger a is, i.e. the farther E-STATCOM is away from the generator, the less influence that P_{inj} and Q_{inj} has on ΔP_g and ΔQ_g. Although for simplicity this is the conclusion obtained under the assumption that cosδ_{g0}, the power factor of generator, is approximate to 1, the following accurate analysis without the assumption verifies the correctness of this conclusion.

Variations of K_x, Γ_x and Φ_x(x = P, Q) *vs.* a, the location of E-STATCOM, can be obtained directly from (5)-(7) and (9)-(11) and are shown in Fig. 4. Fig. 4(a) and (b) are obtained under operating conditions that the active power P_{g0} flowing out of generator is 0.1 p.u. and 0.9 p.u. respectively. Comparison between Fig. 4(a) and (b) shows that the value of P_{g0} has a great influence on K_P and K_Q. However, the value of P_{g0} has little effect on Γ_P and Φ_Q, which decrease linearly from 1 to 0 and are consistent with (14). Besides, Γ_Q is much smaller than Γ_P, which means that Q_{inj} has weaker ability thanP_{inj} to influence ΔP_g. It demonstrates that E-STATCOM, which can supply both active and reactive power, is more powerful in suppressing FOs than devices only injecting reactive power. In conclusion, Fig. 4 indicates that the ability of E-STATCOM to influence P_g and Q_g is little affected by the operating condition, but it's related to the location of E-STATCOM. The smaller a is, namely the closer E-STATCOM is to the generator, the greater ability it has to influence P_g and Q_g.

B. FORCED OSCILLATIONS

FOs are caused by external fluctuating forces in power system. Compared with the fluctuations of loads, the probability and severity of FOs caused by the fluctuation of mechanical power output are much higher [24]. In Fig. 3, ΔP_m is the mechanical power output, the fluctuation of which leads to the FOs ΔP_g and ΔQ_g of generator. Further, it causes the FOs in the system represented by ΔP_b and ΔQ_b. From Fig. 3, the transfer functions from ΔP_m to ΔP_b and ΔQ_b without E-STATCOM are $H_{Pb0}(s)$ and $H_{Qb0}(s)$, respectively:

$$H_{Pb0}(s) = \frac{\omega_b K_P}{Ms^2 + Ds + \omega_b K_P} \tag{15}$$

$$H_{Qb0}(s) = \frac{K_Q}{K_P}H_{Pb0}(s) = \frac{\omega_b K_Q}{Ms^2 + Ds + \omega_b K_P} \tag{16}$$

(15) and (16) indicate that ΔP_b is proportional to ΔQ_b. The natural frequency ω_n of $H_{Pb0}(s)$ and $H_{Qb0}(s)$ is:

$$\omega_n = \sqrt{\frac{\omega_b K_P}{M}} \tag{17}$$

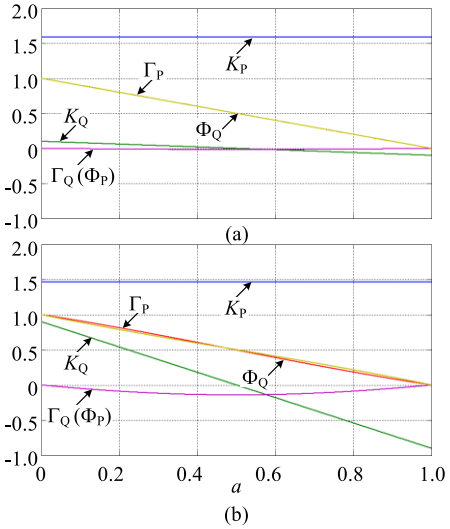

FIGURE 4. Variations of K_x, Γ_x and Φ_x(x = P, Q) vs. the location of E-STATCOM a: (a) the active power flowing out of generator $P_{g0} = 0.1$ p.u., (b) $P_{g0} = 0.9$ p.u.

The damping ratio ξ of $H_{\mathrm{Pb0}}(s)$ and $H_{\mathrm{Qb0}}(s)$ is

$$\xi = \frac{1}{2} D \sqrt{\frac{M}{\omega_{\mathrm{b}} K_{\mathrm{P}}}} \tag{18}$$

If sinusoidal component whose frequency approaches ω_{n} is included in ΔP_{m}, large-amplitude oscillations of ΔP_{b} and ΔQ_{b} occur. This is also shown by the frequency response of $H_{\mathrm{Pb0}}(s)$ and $H_{\mathrm{Qb0}}(s)$ in Fig. 5. The gains of $H_{\mathrm{Pb0}}(s)$ and $H_{\mathrm{Qb0}}(s)$ around ω_{n} are very large, leading to large-amplitude oscillations of ΔP_{b} and ΔQ_{b} only with a small disturbance of ΔP_{m}. Specifically, the gains of $H_{\mathrm{Pb0}}(s)$ and $H_{\mathrm{Qb0}}(s)$ at ω_{n} are

$$\left|H_{\mathrm{Pb0}}\left(j\omega_{\mathrm{n}}\right)\right| = \frac{\omega_{\mathrm{b}} K_{\mathrm{P}}}{D\omega_{\mathrm{n}}} \tag{19}$$

$$\left|H_{\mathrm{Qb0}}\left(j\omega_{\mathrm{n}}\right)\right| = \frac{\omega_{\mathrm{b}} K_{\mathrm{Q}}}{D\omega_{\mathrm{n}}} \tag{20}$$

(19) and (20) are the amplification factors of ΔP_{b} and ΔQ_{b} to ΔP_{m}, respectively. The larger they are, the more serious the FOs will be. (19) and (20) show that although larger damping D could reduce the oscillation amplitude, it cannot fully suppress the oscillations unless the damping is increased to infinite. It explains why FOs still happen even when the system has good damping characteristics. Therefore, breaking free from increasing the damping, a novel method based on E-STATCOM to eliminate FOs is proposed by this paper.

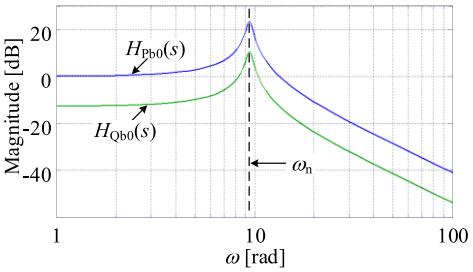

FIGURE 5. Frequency response of $H_{\mathrm{Pb0}}(s)$ and $H_{\mathrm{Qb0}}(s)$ ($a = 0.25$, $P_{\mathrm{g0}} = 0.7$ p.u.).

III. PROPOSED METHOD TO SUPPRESS FORCED OSCILLATIONS

A. KEY IDEA

In Fig. 3, the fluctuation of ΔP_{m} leads to the FOs ΔP_{g} and ΔQ_{g} of generator, and further causes the FOs ΔP_{b} and ΔQ_{b} flowing to the rest of power system. Since to the rest of power system, ΔP_{b} and ΔQ_{b} can be regarded as the disturbance sources which lead to the spread of FOs, they are more harmful. Therefore, suppressing the oscillations of ΔP_{b} and ΔQ_{b} to 0 is chosen as the control object. In order to achieve this object, resonant controllers are adopted to perform closed-loop control on ΔP_{b} and ΔQ_{b}, as shown in Fig. 6. The two resonant controllers have the

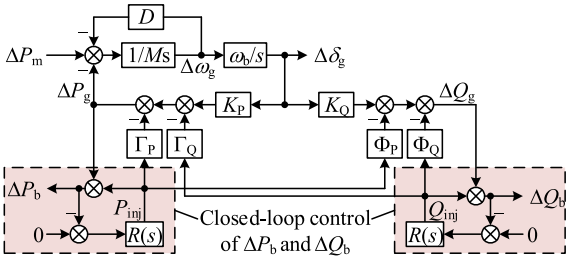

FIGURE 6. Suppression method of FOs based on resonant controller.

same expression:

$$R\left(s\right) = \frac{K_{\mathrm{R}} s}{s^2 + \omega_{\mathrm{c}}^2} \tag{21}$$

where ω_{c} is the central frequency of $R(s)$ and K_{R} is the proportional coefficient. The differences between 0 and ΔP_{b}, ΔQ_{b} are used as the input signals of the two controllers, whose output signals are the reference values of active and reactive power of E-STATCOM separately. The frequency response of $R(s)$ is shown in Fig. 7. (21) and Fig. 7 indicate that the gain of $R(s)$ at ω_{c} is infinite, which is the reason for its good performance in controlling sinusoidal signals. Meanwhile, the gain of $R(s)$ at other frequencies are very small, enabling it to maintain the stability of the system.

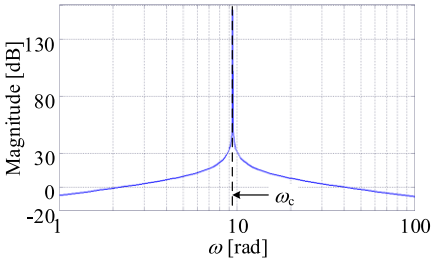

FIGURE 7. Frequency response of of R(s) ($\omega_{\mathrm{c}} = 2\pi \cdot 1.44$, $K_{\mathrm{R}} = 40$).

From the dashed boxes in Fig. 6, with the proposed method, the transfer function $H_{\mathrm{bg}}(s)$ from ΔP_{g} to ΔP_{b} and from ΔQ_{g} to ΔQ_{b} is

$$H_{\mathrm{bg}}\left(s\right) = \frac{\Delta P_{\mathrm{b}}\left(s\right)}{\Delta P_{\mathrm{g}}\left(s\right)} = \frac{\Delta Q_{\mathrm{b}}\left(s\right)}{\Delta Q_{\mathrm{g}}\left(s\right)} = \frac{1}{1 + R\left(s\right)} \tag{22}$$

Since the gain of $R(s)$ at ω_{c} is infinite, (23) can be obtained from (22):

$$\begin{cases} \Delta P_{\mathrm{b}}\left(j\omega_{\mathrm{c}}\right) = \dfrac{1}{1 + R\left(j\omega_{\mathrm{c}}\right)} \Delta P_{\mathrm{g}}\left(j\omega_{\mathrm{c}}\right) = 0 \\ \Delta Q_{\mathrm{b}}\left(j\omega_{\mathrm{c}}\right) = \dfrac{1}{1 + R\left(j\omega_{\mathrm{c}}\right)} \Delta Q_{\mathrm{g}}\left(j\omega_{\mathrm{c}}\right) = 0 \end{cases} \tag{23}$$

It indicates that the oscillations at the frequency of ω_{c} will not be transferred to ΔP_{b} and ΔQ_{b}. Therefore, if the central frequency of $R(s)\omega_{\mathrm{c}}$ is set to the frequency of the disturbance ΔP_{m}, the oscillations of ΔP_{b} and ΔQ_{b} can be eliminated.

It is worth noting that (23) is obtained directly from the dashed box in Fig. 6, which does not involve any assumption of the location of E-STATCOM, the operating condition or structure of the rest of the power system. Therefore, no matter for single-machine or multi-machine system and no matter where the E-STATCOM is installed, (23) is always true. Namely, no FOs will pass through the bus connected with E-STATCOM to the rest of the system. It demonstrates the generality of the proposed method.

This method can be applied to suppress FOs at any frequency by setting the central frequency of $R(s)$ to the frequency of FOs, which can be obtained with parameter identification method of FOs [25]. Since FOs are most serious when the frequency of the disturbance equals to the natural frequency ω_n of the power system, the central frequency of $R(s)$ can also be set to the natural frequency obtained by eigenvalue analysis [26]. Above analysis is based on a general condition without assuming the frequency of FOs. Next, to give a detailed example, the most serious situation is considered and analyzed, where ω_c, the central frequency of $R(s)$, is set to the natural frequency ω_n of power system. In this case, the frequency response of $H_{Pb}(s)$ and $H_{Qb}(s)$, which are the transfer functions from ΔP_m to ΔP_b and ΔQ_b with the proposed method, are obtained from Fig. 6 and depicted in Fig. 8. To make a comparison, the frequency response of $H_{Pb0}(s)$ and $H_{Qb0}(s)$, the transfer functions without the proposed method, are also shown in Fig. 8. It is clear that gains of $H_{Pb}(s)$ and $H_{Qb}(s)$ around ω_n are very small and hence FOs at the frequency of ω_n can be completely eliminated.

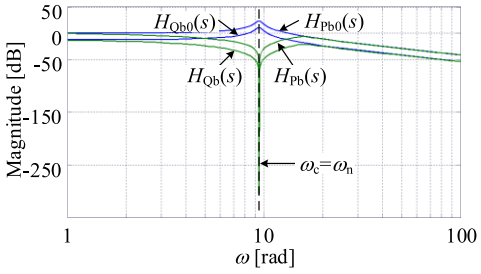

FIGURE 8. Gain characteristics of of $H_{Pb0}(s)$, $H_{Qb0}(s)$, $H_{Pb}(s)$ and $H_{Qb}(s)$ ($a = 0.50$).

B. IMPACT OF E-STATCOM ON THE OSCILLATIONS OF ΔP_g AND ΔQ_g

According to the analysis in Part A, the structure of power system and the location of E-STATCOM do not influence the ability of the proposed method to eliminate the oscillations of ΔP_b and ΔQ_b. Nevertheless, they have effect on the oscillations of ΔP_g and ΔQ_g flowing from the disturbed generator/area to E-STATCOM. This part will analyze it in detail.

Firstly, the influence of the proposed method on ΔP_g is analyzed and the influence on ΔQ_g can be considered in a similar way. Fig. 9 shows the block diagram of the proposed method in a general power system, where $G_{Pg}(s)$ represents

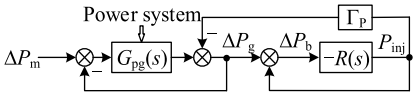

FIGURE 9. Block diagram of the proposed method in a general power system.

the open-loop transfer function from ΔP_m to ΔP_g. According to the analysis in Part A Section II, Γ_Q, the ability of reactive power Q_{inj} injected by E-STATCOM to influence P_g, is very small compared to Γ_P, the ability of active power P_{inj} and hence can be neglected. From Fig. 9, the closed-loop transfer function $H_{Pg}(s)$ from ΔP_m to ΔP_g is

$$H_{Pg}(s) = \frac{G_{Pg}(s)[1+R(s)]}{1+(1-\Gamma_P)R(s)+G_{Pg}(s)[1+R(s)]} \tag{24}$$

Since the gain of $R(s)$ at the frequency of ω_c is infinite, the gain of $H_{Pg}(s)$ at ω_c can be obtained as

$$H_{Pg}(j\omega_c) = \frac{G_{Pg}(j\omega_c)}{1-\Gamma_P+G_{Pg}(j\omega_c)} = \frac{m+jn}{1-\Gamma_P+m+jn} \tag{25}$$

where, m and n denote the real and imaginary part of $G_{Pg}(j\omega_c)$ respectively. Also, the gain of $H_{Pg0}(s)$, the closed-loop transfer function from ΔP_m to ΔP_g without E-STATCOM, at the frequency of ω_c can be obtained with Γ_P set to 0 as

$$H_{Pg0}(j\omega_c) = \frac{m+jn}{1+m+jn} \tag{26}$$

In order to analyze the influence of the proposed method on ΔP_g, the values of $|H_{Pg}(j\omega_c)|$ and $|H_{Pg0}(j\omega_c)|$ are compared. If $|H_{Pg}(j\omega_c)| < |H_{Pg0}(j\omega_c)|$, the oscillations of ΔP_g can be reduced and otherwise cannot. According to (25) and (26), when $1+m$ and Γ_P are of the opposite signs, $|H_{Pg}(j\omega_c)|$ is smaller than $|H_{Pg0}(j\omega_c)|$. Generally, for FOs, $|H_{Pg0}(j\omega_c)|$ is much larger than 1, hence m should be a negative value. At the same time, Γ_P is a positive value based on the analysis in Section II. Therefore, as long as m is smaller than -1, $|H_{Pg}(j\omega_c)|$ will be smaller than $|H_{Pg0}(j\omega_c)|$ and the FOs of ΔP_g can be reduced.

Specifically, a quantitative analysis is performed in SMIB system. The closed-loop transfer function $G_{Pg}(s)$ from ΔP_m to ΔP_g can be obtained from Fig. 3:

$$G_{Pg}(s) = \frac{\omega_b K_P}{Ms^2+Ds} \tag{27}$$

Substituting (27) into (25) can get

$$H_{Pg}(j\omega_c) = \frac{\omega_b K}{\left(-M\omega_c^2+Dj\omega_c\right)(1-\Gamma_P)+\omega_b K} \tag{28}$$

Considering the most serious condition that the frequency of the disturbance equals to the natural frequency of the system ω_n, the central frequency ω_c of $R(s)$ is set to ω_n. In light of $G_{pg}(j\omega_c) = m + jn$ and (27) obtained

in SMIB system, m is obviously smaller than -1. Accordingly, the proposed method is able to reduce the oscillations of ΔP_g.

Substituting (17) and (18) into (28), the amplitude of $H_{Pg}(j\omega_c)$ can be obtained as (29), which is the amplification factor of ΔP_g to the disturbance ΔP_m.

$$\left|H_{Pg}\left(j\omega_c\right)\right| = \frac{1}{\sqrt{\left(1-\Gamma_P\right)^2 B + \Gamma_P^2}} \tag{29}$$

where B is expressed as

$$B = \frac{4\xi^2}{M^2} \tag{30}$$

Based on (29), the derivative of $|H_{Pg}(j\omega_c)|$ with respect to Γ_P is

$$\frac{\mathrm{d}\left|H_{Pg}\left(j\omega_c\right)\right|}{\mathrm{d}\Gamma_P} = \frac{B-(B+1)\Gamma_P}{\left[\left(1-\Gamma_P\right)^2 B + \Gamma_P^2\right]^{3/2}} \tag{31}$$

(31) indicates that if $\Gamma_P \in [0, B/(B+1)]$, $|H_{Pg}(j\omega_c)|$ is an increasing function of Γ_P, while it is a decreasing function of Γ_P when $\Gamma_P \in [B/(B+1), 1]$. Normally, ξ^2 is much smaller than 1 and the range of the inertia of the generator M is [4, 20] [7]. Therefore, the value of B is small and as a result the interval of decrease is short. At the same time, in light of (14), Γ_P is a decreasing function of a. Therefore, $|H_{Pg}(j\omega_c)|$ can be regarded as an increasing function of a, which means that the smaller a is (namely the closer E-STATCOM is to the generator), the smaller amplitude of the oscillations flowing out of the disturbed generator/area is.

Substituting (6) into (29), the variations of $|H_{Pg}(j\omega_c)|$ *vs.* a are obtained as Fig. 10. It shows that when a increases from 0 to 0.5, $|H_{Pg}(j\omega_c)|$ rises slowly from 1 to 2. But when a increases from 0.5 to 1.0, $|H_{Pg}(j\omega_c)|$ goes up rapidly to about 15. Furthermore, it is only affected a little by P_{g0}, which indicates that the performance of proposed method for suppressing ΔP_g is a little affected by the operating condition, but it is primarily decided by the location of E-STATCOM. When a is 1.0, Γ_P equals to 0.0, namely the active power supplied by E-STATCOM P_{inj} has no effect on ΔP_g. In this case, the value of $|H_{Pg}(j\omega_c)|$ equals to that of $|H_{Pg0}(j\omega_c)|$, the amplification factor of ΔP_g to ΔP_m without E-STATCOM. From Fig. 10, it is clear that $|H_{Pg}(j\omega_c)|$ is always smaller than $|H_{Pg0}(j\omega_c)|$. Therefore, wherever E-STATCOM is installed, the proposed method has suppression effect on ΔP_g and it is little affected by the operating condition.

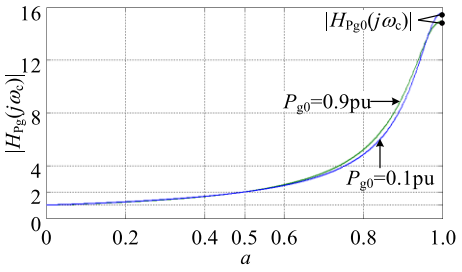

FIGURE 10. The variations of $|H_{Pg}(j\ \omega_c)|$ vs. a with $P_{g0} = 0.1$ p.u. and $P_{g0} = 0.9$ p.u.

As to ΔQ_g, the gain of closed-loop transfer function from ΔP_m to ΔQ_g can be obtained from Fig. 6

$$\left|H_{Qg}\left(j\omega_c\right)\right| = \frac{\left|K_Q\right|}{\left|K_P\right|}\left|H_{Pg}\left(j\omega_c\right)\right| \tag{32}$$

Equation (32) shows that the proposed method has a similar effect on ΔQ_g as ΔP_g. In summary, regardless of the operating condition and the location of E-STATCOM, the proposed method helps to suppress oscillations of ΔP_g and ΔQ_g.

C. CAPACITY OF E-STATCOM

The analysis in Part A demonstrates that the proposed method can eliminate the oscillations of ΔP_b and ΔQ_b spreading from the bus installed with E-STATCOM to the rest of the power system. The following equations can be obtained at steady state:

$$P_{inj}\left(j\omega_c\right) = \Delta P_b\left(j\omega_c\right) - \Delta P_g\left(j\omega_c\right) = -\Delta P_g\left(j\omega_c\right) \tag{33}$$

$$Q_{inj}\left(j\omega_c\right) = \Delta Q_b\left(j\omega_c\right) - \Delta Q_g\left(j\omega_c\right) = -\Delta Q_g\left(j\omega_c\right) \tag{34}$$

Equations (33) and (34) indicate that the active and reactive power injected by E-STATCOM are determined by the active and reactive power flowing out of the disturbed area/generator at the steady state. Hence, the apparent power of E-STATCOM can be obtained as:

$$S_{inj} = \sqrt{P_{inj}^2 + Q_{inj}^2} \tag{35}$$

Considering the transient state, S_{inj} needs to multiply a coefficient larger than 1. According to Fig. 10, the smaller a is (namely the closer E-STATCOM is to the generator), the smaller the oscillations flowing out of the disturbed generator /area are and the smaller capacity of E-STATCOM is required. Since the minimum value of a is larger than 0, the required capacity of E-STATCOM is larger than the power of disturbance ΔP_m. In conclusion, from the aspect of reducing capacity, E-STATCOM should be installed as close as possible to the disturbed generator/area, such as wind farms, charging stations for electric cars and etc.

Above gives the active and reactive power that STATCOM need to provide at steady state. It should be noted that, the capacity obtained with the method in this section is the necessary capacity for suppressing FOs. In practice, E-STATCOM has many other functions, which should also be considered when deciding the capacity.

IV. CASE STUDIES

In this section, we present two case studies of using E-STATCOM to suppress FOs. The first one is a SMIB system, and the second one is the well-known four-machine two-area system. In the two case studies, the performance of the proposed method will be demonstrated with

E-STATCOM installed at different locations and the system operating under distinct conditions.

A. SMIB SYSTEM

A SMIB system shown as Fig. 1 is constructed in Matlab/Simulink, which is rated 13.8/230 kV, 200 MVA. In this system, the active power delivered by transmission line is 0.7 p.u. Since E-STATCOM has the characteristic of current source, the dynamic load model in Matlab/Simulink is adopted, the active and reactive power of which injecting into the network are modulated by the proposed method. A 0.01 p.u. sinusoidal fluctuation at 1.44Hz is included in the mechanical power output from 2s to 17s, which could be caused by vortex related oscillations of hydro turbine or steam pressure fluctuation of steam turbine, to excite FOs [2], [27].

Firstly, we assume that the E-STATCOM is installed at the terminal of the generator, where a is equal to 0.471. The simulation results are shown in Fig. 11. Without the proposed method, the oscillations of ΔP_b and ΔQ_b flowing out of the disturbed generator are 0.14 p.u. and 0.02 p.u., which amplify the disturbance by 14 and 2 times respectively, demonstrating the danger of FOs. By contrast, with the proposed method, ΔP_b and ΔQ_b are eliminated to 0 at steady state, and ΔP_g and ΔQ_g are reduced to 0.019 p.u. and 0.003 p.u. respectively, which is consistent with Fig. 10 and demonstrates the good suppression effect on ΔP_g and ΔQ_g. P_{inj} and Q_{inj} injected by E-STATCOM are shown in Fig. 11(c), which are

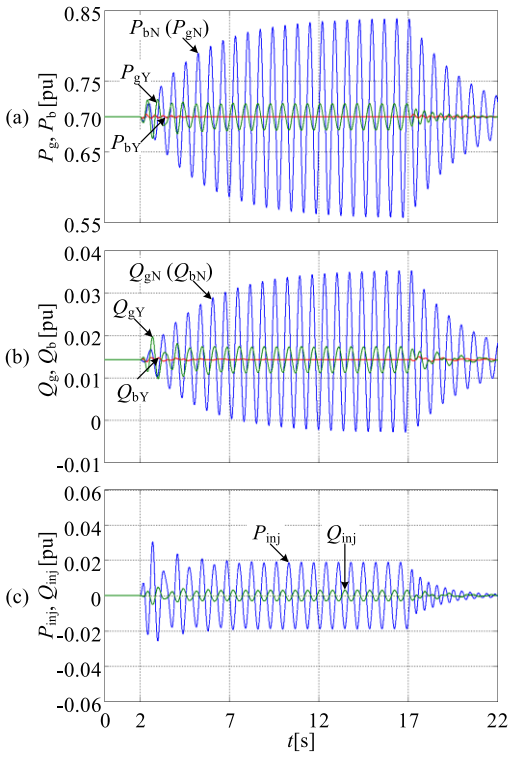

FIGURE 11. Simulation results in SMIB system with $a = 0.471$, where the subscripts Y and N denote the ones with and without the proposed method, respectively.

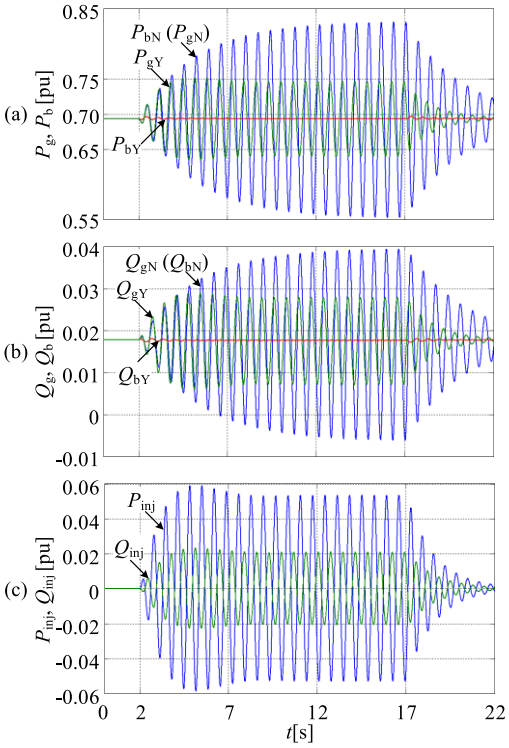

FIGURE 12. Simulation results in SMIB system with $a = 0.873$, where the subscripts Y and N denote the ones with and without the proposed method, respectively.

0.019 p.u. and 0.003 p.u. and equal to ΔP_g and ΔQ_g respectively. Accordingly, the required capacity of E-STATCOM is 3.8 MVA. It indicates that with the proposed method, only a small amount of power is injected by E-STATCOM to achieve a good suppression effect, agreeing well with the theoretical analysis.

Then we assume that E-STATCOM is installed at the middle of the transmission line, where a is equal to 0.873. The simulation results are shown in Fig. 12. Without the proposed method, the oscillations of ΔP_b and ΔQ_b flowing to the infinite bus are 14 and 4 times of the disturbance ΔP_m and so are the oscillations of ΔP_g and ΔQ_g. By contrast, with the proposed method, the oscillations of ΔP_b and ΔQ_b are eliminated to 0. The amplification factors of ΔP_g and ΔQ_g to ΔP_m are reduced to 5.3 and 2 separately. P_{inj} and Q_{inj} injected by E-STATCOM are also 0.053 p.u. and 0.020 p.u., and hence the required capacity is 11.4 MVA.

According to Fig. 11 and Fig. 12, regardless of the location of the E-STATCOM, the proposed method can always eliminate the oscillations of ΔP_b and ΔQ_b, and also reduce the oscillations of ΔP_g and ΔQ_g. But the suppression effect on ΔP_g and ΔQ_g is dependent on the location of E-STATCOM. The closer E-STATCOM is to the source of the disturbance, the greater the suppression effect it has on ΔP_g and ΔQ_g and the smaller capacity of E-STATCOM is needed.

B. FOUR-MACHINE TWO-AREA SYSTEM

In this part, we investigate the effectiveness of the proposed method in the well-known four-machine two-area system [7],

which is rated 20/230 kV, 900 MVA. The structure of the system is depicted in Fig. 13 and the simulations are carried out under two different operating conditions. PSSs are installed to ensure the damping ratio of all oscillation modes are increased to a well-damped level. A 0.01 p.u. sinusoidal fluctuation at 0.60Hz is included in the mechanical power output of G1 from 4s to 34s. E-STATCOM is installed on bus 7.

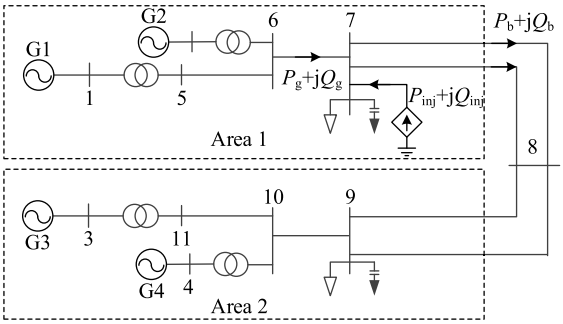

FIGURE 13. The structure of four-machine two-area system.

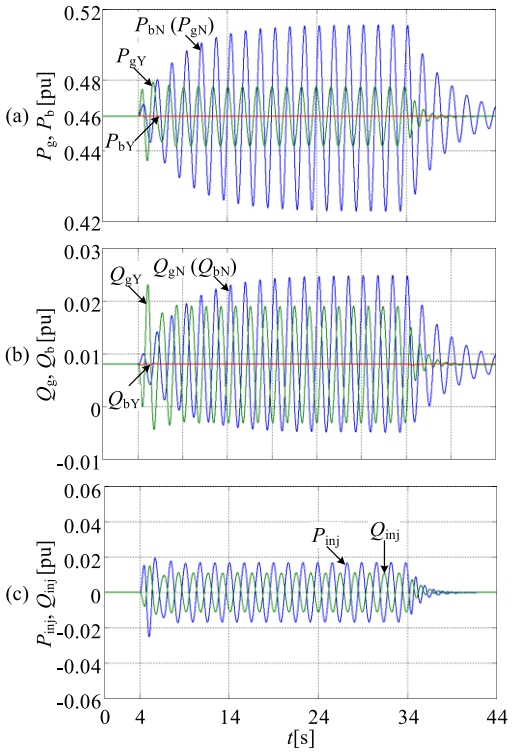

FIGURE 14. Simulation results in four-machine two-area system under operating condition 1, where the subscripts Y and N denote the ones with and without the proposed method, respectively.

Fig. 14 presents the P_g and Q_g flowing from the disturbed area to E-STATCOM, P_b and Q_b flowing to the rest of the system, and P_{inj} and Q_{inj} injected by E-STATCOM. The active power of the four generators P_{gx}(x = 1,2,3,4) are illustrated in Fig. 15 and the amplification factors of them to the disturbance ΔP_m are listed in Table 1. They show

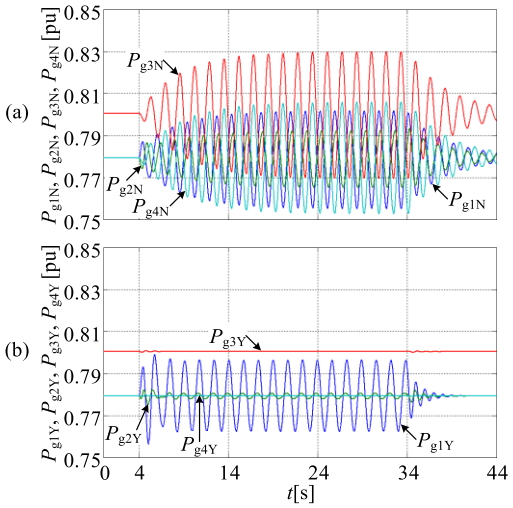

FIGURE 15. The active power of the four generators in the four-machine two-area system under operating condition 1, where the subscripts Y and N denote the ones with and without the proposed method, respectively.

TABLE 1. Amplification factors of oscillations to disturbance ΔP_m in four-machine two-area system under operating condition 1.

	ΔP_b	ΔQ_b	ΔP_g	ΔQ_g	ΔP_{g1}	ΔP_{g2}	ΔP_{g3}	ΔP_{g4}
Without E-STATCOM	5.2	1.7	5.2	1.7	2.2	1.2	3.0	2.6
With E-STATCOM	0	0	1.7	1.1	1.7	0.1	0	0

that large amplitude of FOs still happen even the system is equipped with PSSs and has good damping characteristics, which demonstrate the less effectiveness of improving damping on suppressing FOs. However, with the proposed method, oscillations of P_b and Q_b flowing to area 2 are eliminated, and hence P_{g3} and P_{g4}, the active power of G3 and G4 in area 2, will not contain any oscillation. The active power flowing from Area 1 to E-STATCOM and the oscillations of G2 are also reduced. Yet ΔP_{g1}, the active power oscillations of G1, are not reduced significantly. This is because the electrical distance between E-STATCOM and G1 is relatively long and E-STATCOM has smaller influence on ΔP_{g1}. The active and reactive power P_{inj} and Q_{inj} injected by E-STATCOM are 0.017 p.u. and 0.011 p.u., and accordingly the required capacity is 18 MVA. In summary, with the proposed method, only a small amount of power is required to prevent the FOs spreading from the disturbed area to other areas and to reduce the oscillations in the disturbed area, emonstrating the effectiveness of the proposed method.

Further, the performance of the proposed method is tested when the system is under operating condition 2, where the load in each area changes and causing the transmitted active power from area 1 to area 2 changes from 0.460p.u. to −0.465 p.u. Whereas the location of E-STATCOM, the disturbance and the controller remain the same. The simulation results are shown in Fig. 16. With E-STATCOM, although the operating condition changes significantly, the oscillations of P_b and Q_b flowing to the rest

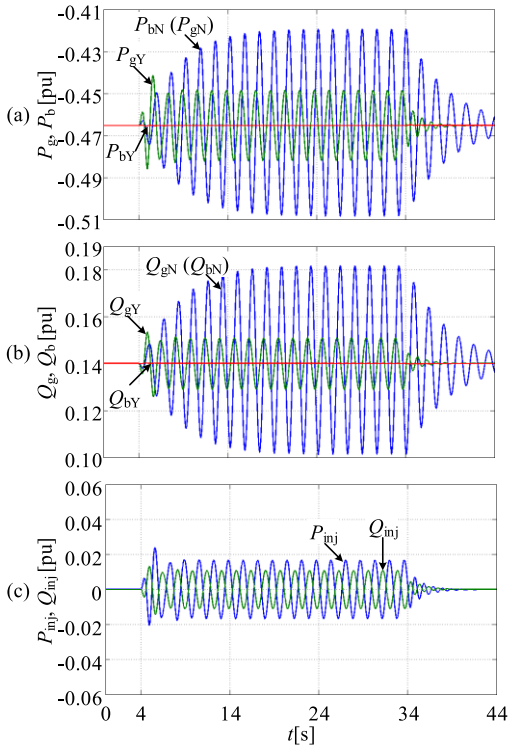

FIGURE 16. Simulation results in four-machine two-area system under operating condition 2, where the subscripts Y and N denote the ones with and without the proposed method, respectively.

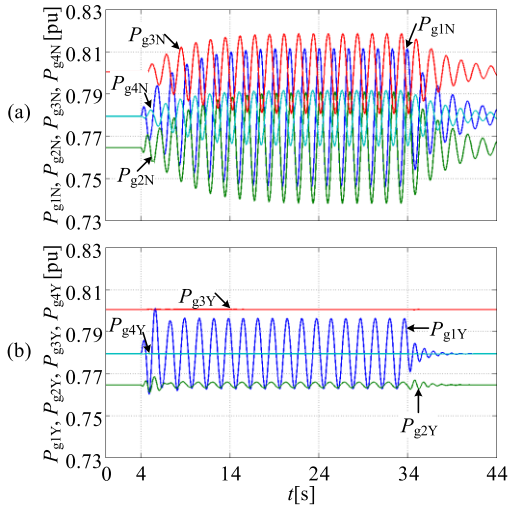

FIGURE 17. The active power of the four generators in the four-machine two-area system under operating condition 2, where the subscripts Y and N denote the ones with and without the proposed method, respectively.

of the system are still fully suppressed. As to the oscillations of generators shown in Fig. 17, P_{g3} and P_{g4} in area 2 are eliminated to 0 and P_{g1} and P_{g2} in the disturbed area are reduced with the proposed method.

To compare the proposed method with the existing method of improving damping, we further increase the damping by increasing the static gain of PSSs to compare the proposed

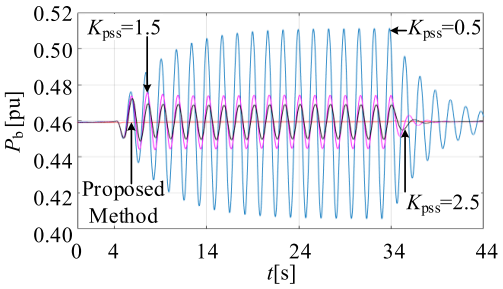

FIGURE 18. Oscillations of P_b when improving the damping and with the proposed method.

method with it. Fig. 18 shows P_b when increasing the damping, where the oscillations with the proposed method are also shown in it for comparison. It can be found clearly that with the increasing of damping, the oscillations of P_b reduce, but are still obvious. According to the theoretical analysis, the oscillations will be zero only when the static gain is infinite, which is not practical considering other oscillation modes of power system. On the contrary, the proposed method eliminates the oscillations of P_b in both conditions. which is consistent with the analysis in Section III.

V. CONCLUDING REMARKS

This paper proposes a novel method that suppresses FOs in power systems by use of E-STATCOM. Resonant controller is adopted to perform a closed-loop control on the active and reactive power flowing from the disturbed generator/area to the rest of the power system, modulating the active and reactive power needed to be supplied by E-STATCOM. It is shown by theoretical analysis and simulation results that the FOs propagating to the rest of the power system are fully suppressed, and the FOs of disturbed generator/area are also reduced. When the location of E-STATCOM is close to the disturbance source, the required capacity of E-STATCOM is relatively small.

In a more complex meshed power grid, the proposed method can not only be applied to E-STATCOM, it is also applicable to energy storage unit/plant by adjusting the active and reactive power to achieve good mitigation effect on FOs. But the location and the coordination of multiple equipment needs to be considered to better suppress FOs in whole power grid. Besides, several resonant controllers can be used in parallel, which is helpful to suppress *multi-mode* FOs and will be further investigated.

REFERENCES

[1] J. Follum and J. W. Pierre, "Detection of periodic forced oscillations in power systems," *IEEE Trans. Power Syst.*, vol. 31, no. 3, pp. 2423–2433, May 2016.

[2] S. A. N. Sarmadi and V. Venkatasubramanian, "Inter-area resonance in power systems from forced oscillations," *IEEE Trans. Power Syst.*, vol. 31, no. 1, pp. 378–386, Jan. 2016.

[3] X. Wang and K. Turitsyn, "Data-driven diagnostics of mechanism and source of sustained oscillations," *IEEE Trans. Power Syst.*, vol. 31, no. 5, pp. 4036–4046, Sep. 2016.

[4] J. Ma, P. Zhang, H.-J. Fu, B. Bo, and Z.-Y. Dong, "Application of phasor measurement unit on locating disturbance source for low-frequency oscillation," *IEEE Trans. Smart Grid*, vol. 1, no. 3, pp. 340–346, Dec. 2010.
[5] M. Ghorbaniparvar, "Survey on forced oscillations in power system," *J. Mod. Power Syst. Clean Energy*, vol. 3, pp. 1–12, Mar. 2016.
[6] K. Sun, "Locating the source of sustained oscillations," presented at the IEEE PES Gen. Meeting, Boston, MA, USA, Jul. 2016.
[7] P. Kundur, *Power System Stability and Control*. New York, NY, USA: McGraw-Hill, 1994.
[8] J. Deng, C. Li, and X. P. Zhang, "Coordinated design of multiple robust FACTS damping controllers: A BMI-based sequential approach with multi-model systems," *IEEE Trans. Power Syst.*, vol. 30, no. 6, pp. 3150–3159, Nov. 2015.
[9] Y. Yu, Y. Min, L. Chen, and P. Ju, "The disturbance source identification of forced power oscillation caused by continuous cyclical load," in *Proc. 4th Int. Conf. Electr. Utility Deregulation Restructuring Power Technol. (DRPT)*, Weihai, Shandong, 2011, pp. 308–313.
[10] X. Wang, X. Li, and F. Li, "Analysis on oscillation in electro-hydraulic regulating system of steam turbine and fault diagnosis based on PSOBP," *Expert Syst. Appl.*, vol. 37, no. 5, pp. 3887–3892, May 2010.
[11] J. D. M. De Kooning, T. L. Vandoorn, J. Van de Vyver, B. Meersman, and L. Vandevelde, "Shaft speed ripples in wind turbines caused by tower shadow and wind shear," *IET Renew. Power Generat.*, vol. 8, no. 2, pp. 195–202, Mar. 2014.
[12] C. Carrillo, A. E. Feijoo, J. Cidras, and J. Gonzalez, "Power fluctuations in an isolated wind plant," *IEEE Trans. Energy Convers.*, vol. 19, no. 1, pp. 217–221, Mar. 2004.
[13] A. Arulampalam, M. Barnes, N. Jenkins, and J. B. Ekanayake, "Power quality and stability improvement of a wind farm using STATCOM supported with hybrid battery energy storage," *IEE Proc.-Generat., Transmiss. Distrib.*, vol. 153, no. 6, pp. 701–710, Nov. 2006.
[14] L. Chen, Y. Min, and W. Hu, "An energy-based method for location of power system oscillation source," *IEEE Trans. Power Syst.*, vol. 28, no. 2, pp. 828–836, May 2013.
[15] T. R. Nudell, S. Nabavi, and A. Chakrabortty, "A real-time attack localization algorithm for large power system networks using graph-theoretic techniques," *IEEE Trans. Smart Grid*, vol. 6, no. 5, pp. 2551–2559, Sep. 2015.
[16] C. Su, W. Hu, Z. Chen, and Y. Hu, "Mitigation of power system oscillation caused by wind power fluctuation," *IET Renew. Power Generat.*, vol. 7, no. 6, pp. 639–651, Nov. 2013.
[17] M. Beza and M. Bongiorno, "An adaptive power oscillation damping controller by STATCOM with energy storage," *IEEE Trans. Power Syst.*, vol. 30, no. 1, pp. 484–493, Jan. 2015.
[18] J. A. Barrado, R. Grino, and H. Valderrama-Blavi, "Power-quality improvement of a stand-alone induction generator using a STATCOM with battery energy storage system," *IEEE Trans. Power Del.*, vol. 25, no. 4, pp. 2734–2741, Oct. 2010.
[19] P. Jiang, S. Feng, and X. Wu, "Robust design method for power oscillation damping controller of STATCOM based on residue and TLS-ESPRIT," *Int. Trans. Elect. Energy Syst.*, vol. 24, no. 10, pp. 1385–1400, Oct. 2014.
[20] A. Hasanzadeh, O. C. Onar, H. Mokhtari, and A. Khaligh, "A proportional-resonant controller-based wireless control strategy with a reduced number of sensors for parallel-operated UPSs," *IEEE Trans. Power Del.*, vol. 25, no. 1, pp. 468–478, Jan. 2010.
[21] J. G. Hwang, P. W. Lehn, and M. Winkelnkemper, "A generalized class of stationary frame-current controllers for grid-connected AC–DC converters," *IEEE Trans. Power Del.*, vol. 25, no. 4, pp. 2742–2751, Oct. 2010.
[22] L. Herman, I. Papic, and B. Blazic, "A proportional-resonant current controller for selective harmonic compensation in a hybrid active power filter," *IEEE Trans. Power Del.*, vol. 29, no. 5, pp. 2055–2065, Oct. 2014.
[23] F. Tang, B. Wang, and Q. Liao, "Research on forced oscillations disturbance source locating through an energy approach," *Int. Trans. Elect. Energy Syst.*, vol. 26, no. 1, pp. 192–207, 2016.
[24] Z. Han, R. He, J. Ma, and Y. Xu, "Comparative analysis of disturbance source inducing power system forced power oscillation," *Autom. Electr. Power Syst.*, vol. 33, no. 3, pp. 16–19, Feb. 2009.
[25] J. Follum, J. W. Pierre, and R. Martin, "Simultaneous estimation of electromechanical modes and forced oscillations," *IEEE Trans. Power Syst.*, vol. 32, no. 5, pp. 3958–3967, Sep. 2017.
[26] C. Liu, X. Li, P. Tian, and M. Wang, "An improved IRA algorithm and its application in critical eigenvalues searching for low frequency oscillation analysis," *IEEE Trans. Power Syst.*, vol. 32, no. 4, pp. 2974–2983, Jul. 2017.
[27] H. Zhiyong, H. Renmu, and X. Yanhui, "Effect of steam pressure fluctuation in turbine steam pipe on stability of power system," in *Proc. 3rd Int. Conf. Electr. Utility Deregulation Restructuring Power Technol.*, Nanjing, China, 2008, pp. 1127–1131.

SHUANG FENG received the B.Sc. degree in electrical engineering from the Nanjing University of Aeronautics and Astronautics, Nanjing, China, in 2012, and the Ph.D. degree in electrical engineering from Southeast University, China, in 2017. She was a Visiting Researcher with the Department of Electrical and Computer Engineering, Texas A&M University, from 2015 to 2016. She is currently a Lecturer with the School of Electrical Engineering, Southeast University. Her research interests include power system stability and control and data analysis of phasor measurement unit.

XI WU received the B.Eng. and Ph.D. degrees in electrical engineering from Southeast University, Nanjing, China, in 2008 and 2013, respectively. He is currently an Associate Professor with the School of Electrical Engineering, Southeast University. His research interests include power system stability and control, smart grid, and renewable energy technology.

PING JIANG received the B.E. from Southeast University, Nanjing, China, in 1982, the M.Eng. degree from the PLA University of Science and Technology, Nanjing, China, in 1988, and the Ph.D. degree from Southeast University, Nanjing, China, in 2010, all in electrical engineering. He is currently a Professor with the School of Electrical Engineering, Southeast University. His research interests include power system stability and control, the application of power electronics in power systems and renewable energy integration.

LE XIE (M'10–SM'16) received the B.E. degree in electrical engineering from Tsinghua University, Beijing, China, in 2004, the M.S. degree in engineering sciences from Harvard University, Cambridge, MA, USA, in 2005, and the Ph.D. degree from the Electric Energy Systems Group, Department of Electrical and Computer Engineering, Carnegie Mellon University, Pittsburgh, PA, USA, in 2009. He is currently an Associate Professor with the Department of Electrical and Computer Engineering, Texas A&M University, College Station, TX, USA, where he is affiliated with the Electric Power and Power Electronics Group. His research interests include modeling and control of large-scale complex systems, smart grid applications in support of renewable energy integration, and electricity markets.

JIAXING LEI (S'14–M'17) received the B.Sc. and Ph.D. degrees in electrical engineering from the College of Automation Engineering, Nanjing University of Aeronautics and Astronautics, Nanjing, China, in 2012 and 2017, respectively. From 2015 to 2016, he was a Visiting Researcher with the Power Electronics, Machines and Control Group, University of Nottingham, Nottingham, U.K. In 2017, he joined Southeast University, where he has been a Lecturer with the School of Electrical Engineering. His research interests include matrix converter and its application in offshore wind energy system and vehicle to grid system.